. **LA-UR** -87-2977

CONF-8708141--1

LA-UR--87-2977

DE88 000507

Los Alamos National Laboratory is operated by the University of California for the United States Department of Energy under contract W-7405-ENG-36

TITLE

PARTICLE INJECTION AND COSMIC RAY ACCELERATION AT COLLISIONLESS PARALLEL SHOCKS

AUTHOR(S) KEVIN B. QUEST, X-1

SUBMITTED TO Proceedings of the Solar Wind Six Meeting
Estes Park, Co., August 24-28, 1987

DISCLAIMER

Los Alamos National Laboratory
Los Alamos, New Mexico 87545

Particle Injection and Cosmic Ray Acceleration at Collisionless Parallel Shocks

K. B. Quest

Inertial Fusion and Plasma Theory, MS-E531
Applied Theoretical Physics Division
Los Alamos National Laboratory
Los Alamos, NM 87545

Abstract

The structure of collisionless parallel shocks is studied using one-dimensional hybrid simulations, with emphasis on particle injection into the first-order Fermi acceleration process. It is argued that for sufficiently high Mach number shocks, and in the absence of wave turbulence, the fluid firehose marginal stability condition will be exceeded at the interface between the upstream, unshocked, plasma and the heated plasma downstream. As a consequence, nonlinear, low-frequency, electromagnetic waves are generated and act to slow the plasma and provide dissipation for the shock. It is shown that large amplitude waves at the shock ramp scatter a small fraction of the upstream ions back into the upstream medium. These ions, in turn, resonantly generate the electromagnetic waves that are swept back into the shock. As these waves propagate through the shock they are compressed and amplified, allowing them to non-resonantly scatter the bulk of the plasma. Moreover, the compressed waves back-scatter a small fraction of the upstream ions, maintaining the shock structure in a quasi-steady state. The back-scattered ions are accelerated during the wave generation process to 2-4 times the ram energy and provide a likely seed population for cosmic rays.

1. Introduction

During the last decade it has been argued that a plausible model for the generation of cosmic rays is first-order Fermi acceleration at collisionless shocks. In the argument's simplest form, low-frequency electromagnetic fluctuations (such as Alfvén waves) are compressed and slowed as they propagate from a position upstream of a collisionless shock to a position downstream. Supra-thermal ions scattering off of these waves conserve energy in the wave rest frame. If the phase speed of the waves is much slower than the local plasma flow speed, it follows that the ions "see" converging mirrors, and particle energization can result. It has been shown that given an initial distribution of moderately energetic ions (a "seed" population), the spectral index of the ions (after acceleration) can be predicted using statistical or test particle arguments, independent of the wave scattering mechanism (Axford et al., 1977; Bell, 1978; Blandford and Ostriker, 1978). Recent reviews of the theory and its application to space and astrophysical plasmas can be found in Axford (1981a,b,c), Blandford and Cowie (1982), Drury (1983), Forman and Webb (1985), Kennel et al. (1985), Scholer (1985), and Blandford and Eichler (1987).

An unresolved issue crucial to the first-order Fermi process is how ions are initially drawn from the thermal background, that is, what is the source and composition of the "seed" population. One possibility is that ions are accelerated up out of the thermal background by some mechanism independent of the shock or the first-order Fermi process, followed by further acceleration to cosmic ray energies by the Fermi mechanism. Candidate processes such as second-order Fermi acceleration and magnetic pumping are discussed in Melrose (1980) and will not be repeated here. Another possibility is shock-shock acceleration, where ions bounce between two (or more) converging shocks and is a variant of the first-order Fermi process (Parker, 1958). It is possible to strongly accelerate ions at nearly perpendicular shocks by either the shock-drift mechanism (Armstrong, 1985) or shock-shock interactions (Cargill et al., 1986). Finally, magnetospheres provide a wealth of possible acceleration mechanisms such as reconnection, double layers, and wave-particle interactions (Arons et al., 1979).

An alternative is that the seed population is provided by the shock dissipation process. This idea is appealing because it eliminates the need for additional (external) processes working in conjunction with the shock acceleration mechanism, and as a consequence, wherever there are shocks there will be the production of cosmic rays. It does imply, however, that shock structure and energetic particle acceleration are inter-dependent, that is, the physics of one will almost certainly affect the other (Blandford and Eichler, 1987).

It is the purpose of this paper to outline a model of collisionless, high Mach number parallel shock structure, and show that the dissipation process requires the generation of electromagnetic waves upstream of the shock, and the scattering and energization of a small fraction of the background ions. These are the same requirements for the initiation of cosmic ray production, and it will be argued that Fermi acceleration is a likely consequence of the model.

2. Parallel Shock Model

In this section a mechanism by which parallel shocks dissipate energy at parallel Mach numbers will be outlined. More details can be found in Quest (1987), on which the following discussion is based.

Collisionless parallel shocks have long been a "problem child" of plasma physics, principally because of the difficulty of propagating nonlinear sound waves along the magnetic field-aligned direction. Viewed from classical collisional hydrodynamics, shock waves are formed when the tendency of compressive waves to steepen are balanced by viscous dissipation. This argument can be generalized to collisional MHD by including dispersion as an alternate way of limiting shock steepening. A problem arises, however, when trying to apply this argument to parallel shock formation in a collisionless medium. First, sound waves are strongly damped unless the upstream ratio of the ion temperature to the electron temperature T_i/T_e is very small (Fried and Gould, 1961). Quasi-linear theory and particle simulations have shown that unless $T_i/T_e < 0.2$, ion acoustic waves are strongly Landau damped and do not steepen to form shocks (Mason, 1970,1971). Second, when the temperature ratio is small enough to support acoustic shocks, there is an upper critical acoustic Mach number between 1.6 to 3 (depending on the electron equation of state).

above which the ion distribution function bifurcates and an increasingly large fraction of the ions are electrostatically reflected back upstream (Moiseev and Sagdeev, 1963; Forslund and Freidberg, 1971; Tidman and Krall, 1971). Such a distribution is strongly unstable to electromagnetic wave growth, implying that, at best, nonlinear acoustic waves will exist only for a limited Mach number range. Finally, parallel propagating Alfvén waves are non-compressive, and do not steepen to form shocks (Kantrowitz and Petschek, 1966). If the sound wave is strongly damped, it is not obvious how a parallel shock can be formed by the steepening arguments.

Parker (1961) reasoned that at sufficiently high Mach numbers a parallel shock will form because the interface where the upstream and downstream plasmas overlap will be unstable to growth of a hose instability. When two or more plasma populations of differing velocity parallel to the background magnetic field inter-penetrate, an effective pressure

$$P_{\parallel} = \sum_{\alpha} N_{\alpha} M_{\alpha} U_{\parallel \alpha}^2 \tag{1}$$

is generated. In (1), the sum is over all species α. N, M, and $U_{\parallel}$ are the density, mass, and parallel bulk velocity, respectively, and the pressure $P_{\parallel}$ is calculated in the electron rest frame (center of mass frame). Assuming for simplicity that the thermal pressures are isotropic, the plasma is unstable to growth of right-hand circularly polarized waves if

$$P_{\parallel} > \frac{B^2}{4\pi}, \tag{2}$$

where B is the magnitude of the background magnetic field. The criterion (2) is completely analogous to the more usual firehose marginal stability condition (Chandrasekhar et al., 1958), where the pressure anisotropies are thermal as opposed to generated by multi-streaming ion beams. In both cases, the plasma is unstable when the centrifugal forces generated by the anisotropies exceed the stabilization due to the magnetic tension.

In interplanetary space, a high speed stream overtaking a slower stream will couple and form a shock if criterion (2) is exceeded. If an obstacle is placed in the flow of a moving plasma, such as the earth's magnetosphere in the solar wind, then plasma reflecting from the obstacle will be unstable, and again a shock will form. Thus, shock formation by the steepening of sound waves is replaced by the coupling of multiple ion beams due to the hose instability (Quest, 1987).

Further illustration of the idea can be provided by the following example. Assume for the moment that two plasmas separated by a discontinuity satisfy the usual Rankine-Hugoniot jump conditions for a parallel shock. As time progresses, will the discontinuity develop into a shock layer that can heat the plasma and provide the necessary dissipation for the wave to be self-consistent? A probable answer is provided in Figure 1.

In Figure 1. the $V_x - x$ phase space and B_y magnetic field component for a parallel shock are shown for 6 succeeding times. The velocities are normalized to the shock ram speed U_s, and the magnetic field is normalized to the background field B_u. The numbers at the right of the figures are the times in units of inverse ion cyclotron frequency Ω_i^{-1}. The shock normal and the background magnetic field are both assumed to be in the x direction. The nominal Alfvén Mach number is 5, the upstream plasma β is 1.5, and

the upstream temperature ratio T_i/T_e is 0.5. The results have been generated by a one-dimensional hybrid code in which the electrons are treated as an isentropic fluid and the ions as macro-particles (Harned, 1982), but for the purposes of discussion the figures can be assumed to be schematics.

At time t=0 the upstream and downstream plasmas are separated by a discontinuity as described above. The transverse magnetic field is 0, consistent with the assumption of no wave fields. As time progresses, the faster, unshocked, plasma overtakes the slower, shocked plasma, creating an unstable interface region. Large amplitude transverse B fields are generated and couple the upstream and downstream plasmas. At late times a shock layer has formed and the plasma transition from upstream to downstream is now self-consistent.

In the following sections the time-asymptotic steady-state structure as predicted by the simulation code will be examined. Before proceeding to this discussion, however, it would be useful to know for what Mach numbers and upstream conditions the hose instability is expected to strongly drive the shock. A simple estimate can be made in the following way: Assume that for small Mach numbers the electrons behave as an isentropic fluid, with ratios of specific heat of 5/3. The justifcation for this assumption is that the long wavelength modes expected from the hose instability will not strongly heat the electrons, and any anisotropies that build up will be quickly smoothed by electron Weibal instabilities. Next, assume that all the irreversible shock heating goes into the ions, and that the heating is one-dimensional, in the shock normal direction. If ion acoustic waves are causing the shock, then the assumption of one-dimensionality is easy to justify. If the temperature ratios are too large to support such waves, then the dimensionality of the shock will depend on the nature of the low Mach number dissipation mechanism, for example, weakly resonant ion beam-driven modes (Quest, 1987). In any event, the assumption of one-dimensionality will provide a lower bound in Mach number for when the firehose condition is first exceeded (see below).

As the Mach number of the shock is increased, the downstream ion temperature ratio $T_{\perp i}/T_{\parallel}$, will increase, since the irreversible heating is going into the parallel direction alone. For sufficiently large Mach numbers, the marginal firehose condition

$$P_{\parallel d} - P_{\perp d} = \frac{B^2}{4\pi} \tag{3}$$

will be exceeded downstream of the shock, assuming a one-dimensional ion compression. For these Mach numbers, the self-consistently generated turbulence should adjust itself so that ions are heated in the perpendicular direction as well as parallel, so that condition (3) is satisfied. Put differently, plasmas downstream of a parallel shock that exceed the criterion (3) will be firehose unstable, and the effect of the instability will be to drive the anisotropies back to criterion (3).

In Figure 2, the minimum Mach number for which the firehose criterion is attained downstream is plotted as a function of upstream plasma β. The assumed T_i/T_e upstream is 0.5, although the results are relatively insensitive to this parameter. In the upper panel the magnetosonic Mach M_s number is plotted, while in the lower panel the Alfén Mach number M_A is used. The shaded areas in the plots correspond to switch-on shocks (lower-left corner) and sub-sonic flow (right corner of Fig 2a). See Quest (1987) for more details.

As can be seen, the firehose condition is achieved for moderate Mach numbers, so that both astrophysically and within the earth's solar system it should be possible to find firehose driven shocks.

3. Shock Structure

In the previous section it was shown that for sufficiently large Mach numbers low-frequency electromagnetic waves are expected as part of the parallel shock structure. The reasons are the lack of an electrostatic sound wave and because the beam-driven marginal firehose condition would otherwise be grossly exceeded. What has not been determined is the structure of these waves. Clearly, they must strongly scatter the bulk of the ions to achieve the necessary shock dissipation, and they must do so in a way such that the marginal firehose condition is satisfied a few thermal gyro-radii downstream of the shock. Within these constraints, however, the wave structure is arbitrary.

Linear theory offers insight as to the expected wave structure. When two or more ion beams inter-penetrate along the magnetic field-aligned direction, there are in general three distinct modes that will be driven unstable. The first is the non-resonant fluid mode discovered simultaneously by Parker (1961) and Kovner (1961). Simulations (Winske and Leroy, 1983) have shown that when this mode is dominant (i.e., exceeds criterion (2)), the wave field grows up until it is strong enough to trap the beams and force them together. An example of this behavior can be seen in Figure 2, where the magnetic field of the wave grows to several times the magnitude of the background field, dominating the motion of the ions, and forcing the two beams to move together. The polarization of this wave is right-handed, and the mode propagates in a direction opposite that of the beam in the center of mass frame (where the "beam" is defined as the ion species with the lower density).

Another mode that can be destabilized is a low-frequency ($< \Omega_i$) electromagnetic wave that cyclotron-resonates with the beam (Kovner, 1961), that is, satisfies at maximum growth the condition

$$\omega - kU_b + \Omega_i \simeq 0, \tag{4}$$

where ω is the complex frequency of the wave, k is the wavenumber, and U_b is the beam velocity in the field aligned direction. This instability has been studied extensively both theoretically (Barnes, 1970; Bell, 1978; Gary, 1978; Achterberg, 1983) and numerically (Winske and Leroy, 1983) and are believed to be at least partially responsible for the observed ion beam structure seen upstream of the earth's bow shock (Sentman et al., 1981; Gary, 1981; Lee, 1982; Thomsen, 1985; and see the special "ISEE Upstream Waves and Particles" issue of the Journal of Geophysical Research, number A6, vol. 86, 1981, and references therein) The waves pitch-angle scatter the beam ions, although non-linear effects can occur for sufficiently strong beams (Winske and Leroy, 1983; Zachary, 1987) The polarization of this mode, like the non-resonant firehose wave described above, is right-handed, but the wave propagates in the direction of the ion beam in the center-of-mass frame.

The third mode is a high frequency ($> \Omega_i$) resonant whistler instability similar to the low-frequency ion mode, but occurs at much shorter wavelengths. This instability interacts

primarily with electrons, and because the unstable bandwidth is small, is unlikely to be an efficient scatterer of ions (Blandford and Eichler, 1987).

Given the above possibilities, which is most likely to describe the shock structure? Parker (1961) envisioned the parallel shock to consist of a quasi-linear wave precursor due to ions "evaporating" from the shock, followed by a region of nonlinear disorder where the main shock transition occurred. The turbulence in the wave precursor is generated by the non-resonant firehose instability, and the far upstream plasma state asymptotes to the marginal firehose condition.

Golden et al. (1973) pursued the idea of ion-beam generated dissipation but argued that the most unstable modes would be those which could group-stand in the shock frame. By using a Mott-Smith superposition as a model for the shock layer (Mott-Smith, 1951), they showed that the high-frequency whistler modes could unstably group-stand within the shock layer for Alfvén Mach numbers greater than 5.5. A problem with this model, however, is that it is not clear how such a high frequency mode can strongly interact with the ions, as is necessary for shock dissipation. Further, the band-width of the instability is very narrow and the waves are likely to saturate at very small amplitudes (Blandford and Eichler, 1987; Quest, 1987).

Jackson (1983) argued that the high Mach number parallel shock consists of an acoustic subshock that reflects a small fraction of the incident ions, and that the low-frequency resonant beam-driven instability is responsible for the subsequent scattering and generation of the upstream diffuse ions. The difficulty of generating the subshock is circumvented by assuming that enough momentum is transferred to the reflected ions so that the effective Mach number at the ramp is below the critical cutoff. This assumption is questionable, particularly for very strong shocks, and still leaves the problem of the upstream temperature ratio, which normally does not satisfy the condition $T_i/T_e < 0.2$.

In an astrophysical context, it has been suggested that whatever mechanism is responsible for the first-order Fermi process (the non-resonant firehose or low-frequency resonant beam-driven modes) might also be responsible for the shock dissipation (Eichler, 1979; Ellison and Eichler, 1984). Thus high-energy Fermi acceleration and shock dissipation can be viewed as the two limits of a spectrum of scattering waves. In Eichler (1979), it was argued that since the scattering length due to the resonant beam instability is a function of energy and can be estimated from quasi-linear theory (Bell, 1978), higher energy particles will extend further upstream of the shock, see less of a slowing of the incident plasma, and therefore be preferentially accelerated. Using this argument, it was shown that a tiny fraction of ions are drawn from the thermal background in such a way as to satisfy the jump conditions across the shock and to compensate for the loss of cosmic rays as they are convected downstream. Interestingly, it was concluded that up to one-half the post shock pressure can be due to the cosmic rays. In our solar system there is insufficient time and size for a shock to accelerate particles to such high energies, but the underlying idea that the dissipation mechanism and the acceleration mechanism are essentially the same should still be true. Ellision and Eichler (1984) and Ellison (1985) developed a Monte-Carlo extension of the analytic model of Eichler (1979) and obtained reasonable agreement with observed energetic particle spectra at the earth's bow shock, providing further plausibility for the model.

4. Hybrid Simulation Results: $M_A = 5$

In this section the structure of a $M_A = 5$, $\beta = 1.0$, and $T_i/T_e = 0.5$ parallel shock, as predicted by a one-dimensional hybrid simulation code, will be examined. The numerical method employed models the ions as a large number (> 24000) of macro-particles, so ion kinetic effects such as bifurcation and resonances are retained. The electrons are modeled as a massless non-resistive fluid with a polytropic equation of state. The plasma is assumed quasi-neutral, so the electron and charge densities are equal. The ratio of specific heats is assumed to be 5/3. The code is electromagnetic, but does ignore the displacement current in Ohm's Law. All three components of the fields and particle velocities are retained, and the system is assumed to depend on one spatial dimension (x). Details of the field solver used in the code can be found in Harned (1982), and applications of similar codes to quasi-parallel shocks may be found in Kan and Swift (1983), Quest (1985), and Thomas and Brecht (1985).

The shock is created by continuously injecting plasma into the simulation box at the left-hand boundary, and specularly reflecting the ions at the right-boundary. This creates a counter-streaming ion beam of density equal to the incident plasma. The beam-firehose criterion (2) is exceeded and the two beams are coupled together by the non-resonant hose instability (see Figure 7 of Quest, 1987).

The late time ($t = 200\Omega_i^{-1}$) ion-phase space is displayed in Figure 3. Figure 3a shows V_x vs. x for the macro-particle ions. The velocity is normalized to the shock speed U_s, and x is normalized to the upstream ion inertial length c/ω_{pi}. The laboratory (simulation) frame is used, so that the average downstream velocity in the x direction is 0. In Figures 3b and 3c, the V_y and V_z phase space for the ions are shown, respectively. The main shock ramp can be identified in Fig 3a as the location where the ion bulk velocity appreciably slows and the temperature increases ($x \simeq 310c/\omega_{pi}$). Coincident with the slowing and heating in x is the beginning of large amplitude transverse oscillations (Figures 3b and 3c). A small number of energetic ions, well separated in velocity space from the background ions can be seen upstream of the main shock transition in all three velocity components.

A rough picture that emerges from Figure 3 is that the shock structure consists of three distinct regions: an upstream foreshock populated by a small number of energetic ions and small transverse oscillations in the plasma, a relatively thin ramp over which the ions are heated and large amplitude wave motion is generated, and a post-ramp plasma which exhibits large oscillations in the transverse direction. Given that the oscillations are transverse, it follows that electromagnetic waves are obviously important to the shock structure. This point is verified in Figure 4.

The transverse B field components (B_y and B_z) are plotted as a function of position for time $t = 200\Omega_i^{-1}$ in Figures 4a and 4b, and are normalized to the upstream field B_u. The magnitude of the wave field $B_w \equiv (B_y^2 + B_z^2)^{1/2}$ is plotted in Figure 4c. Consistent with the previous figure, wave activity is seen both upstream and downstream of the nominal shock position. The wave amplitude increases steadily as the shock is approached from upstream, followed by a large jump in amplitude at the ramp, and then finally decreases many wavelengths downstream. The dominant wavelength upstream is seen to be several times larger than the wavelength downstream (as has been verified by Fourier analyzing

the wave spectrum).

In Figure 5, two components of the ion phase space, the density, and one component of the transverse magnetic field are shown, plotted as a function of position at time $t = 200\Omega_i^{-1}$. All normalizations are the same as in Figures 3 and 4, and the ion density N is normalized to the upstream ion density N_u. The purpose of Figure 5 is to take a closer look at the shock ramp by using a expanded spatial scale. The ions slow and the density increases over a distance of approximately $x \simeq 15c/\omega_{pi}$. The large amplitude transverse waves and the change in wavelength at the shock can be seen in both V_y and B_y. As is expected for an Alfvénic disturbance, the velocity and wave fields are approximately in phase. Notable is the rapid increase in the magnetic field magnitude, which occurs on a scale even smaller than the downstream wavelength of the magnetic field oscillations.

Several runs in addition to $M_A = 5$ have been performed over a range in Mach numbers from approximately 1 to 10. The results have been compared against the predictions of Rankine-Hugoniot jump relations, appropriately modified to include the effects of ion anisotropy, and the wave magnetic fields have been Fourier analyzed in space and time both upstream and downstream of the shock ramp. The interpretation given below has therefore been extensively tested, and found to be in good agreement with the simulations. Details may be found in Quest (1987).

5. Interpretation of High Mach Number Simulation Results

At high Mach numbers (defined as strongly exceeding the marginal stability condition displayed in Figure 2), a self-sustained wave generation process is set up that provides for the necessary dissipation, and at the same time keeps the shock everywhere at the marginal firehose condition or below it. Starting at the main shock transition where large amplitude waves are assumed to exist, a small fraction of the incident ions are reflected-scattered back into the upstream medium. The number of ions is too small to destabilize the non-resonant beam driven firehose (criterion 2), but is large enough to destabilize the resonant ion beam-driven mode, and as such, generate low-frequency, transverse electromagnetic oscillations. In the process of generating the upstream waves the ions are resonantly scattered back towards the shock. Because energy is conserved in the wave frame, and assuming that the waves are slow relative to the upstream flow speed, the scattered ions gain energy in the shock-stationary frame.

As the magnetic oscillations convect back toward the shock, they are amplified and compressed in wavelength. These amplified waves interact strongly with the ions, splitting the distribution into two components. A tiny fraction ($\simeq 2 - 6\%$) are back-scattered (reflected?) at the ramp back into the upstream medium. These ions are necessary to maintain that part of the dissipation process that continuously generates the upstream waves. The remainder of the ions are scattered and slowed by the waves, resulting in the generation of a large downstream temperature, and in coherent transverse motion in phase with the magnetic field.

The irreversible heating is a consequence of several factors. First, the resonant interaction of ions just upstream of the ramp results in partial ion thermalization. Second, as the wave magnetic field continues to amplify and compress (in wavelength), the turning

radius of the majority of the ions ($\simeq U_u/\Omega_w$, where Ω_w is the ion cyclotron frequency based on the magnitude of the wave magnetic field) approaches the wavelength of the wave, and the particle orbits become chaotic. Small differences in the initial particle phase and position results in very different trajectories, heating the plasma. Finally, large electrostatic potentials can and do exist within the shock ramp (see, for example, Figure 18 in Quest, 1987), but their effect on the plasma is unclear. The forces on the ions are a combination of electric and $\mathbf{V} \times \mathbf{B}$ contributions, and the two tend to cancel, reducing the field-aligned potential drop (see, for example, arguments in Goodrich and Scudder, 1985). In a perpendicular shock, the ions that are transmitted move at a speed different from the bulk ion speed (transmitted plus reflected component). Because of this difference, there is a substantial net electromagnetic force on the ions. In a parallel shock, only a very small fraction of the ions are strongly scattered and accelerated, and the net $\mathbf{E} + \mathbf{V} \times \mathbf{B}/c$ is reduced.

The density scale length of the main shock ramp should be the ion turning distance in the compressed wave field ($\simeq 1 - 2U_u/\Omega_i$), and this prediction is in good agreement with the simulation results. The expected scale length of the magnetic ramp is less clear, since the field and density are not constrained to vary together, as they are in the case of a perpendicular shock. Figure 5 shows a magnetic ramp which is smaller than the wavelength of the large amplitude downstream oscillation. Whether this is a consistent feature and indicates that resistive or thermal ion-Larmor-radius scales determine the length of the magnetic jump, or whether the observed jump is simply a transient, is not clear. An additional complication is that for quasi-parallel (as opposed to true parallel) shocks a time-independent jump in the magnetic field could add yet a third spatial spatial scale to the ramp.

A interesting feature of the high Mach number shock simulations is that the resonant beam-driven instability dominates the structure both upstream of and downstream from the main ramp, and the non-resonant mode is not observed (except at early times during shock creation). The reason for the lack of the non-resonant mode downstream is the efficiency of the ion scattering at the shock ramp. The ions are thermalized in 1-2 downstream wavelengths and are never permitted to generate a large anisotropy at the overlap between the upstream and downstream plasmas. Thus, given the amplification of the upstream waves as they cross the shock, there is no need for local wave generation downstream. A possible reason for the number of back-scattered ions not exceeding the firehose condition upstream of the shock is the difficulty in maintaining a steady state. If the marginal state is exceeded, the dispersive properties of the mode changes, resulting in reduced acceleration efficiencies (because of the higher phase speed of the wave) and in strong non-resonant interactions, resulting in a disruption and rapid assimilation (into the background plasma) of the beam. In addition, energy that would have been transferred to the small population of scattered ions is now given to the background ions, further reducing the acceleration efficiency. It does present a constraint at very high Mach numbers, however, because if the marginal firehose condition is not exceeded by the upstream beam, then either a very large anisotropy of the sign $T_\perp \gg T_\parallel$ is created upstream of main ramp, or the number density of the reflected ions must scale as M_A^{-2} (Parker, 1961). Thus (barring a large anisotropy), the number of ions initially injected into the acceleration process will decrease as a function

of increasing shock speed, that is

$$\frac{N_r}{N_u} \propto M_A^{-2}. \tag{5}$$

Unless the spectral index of the Fermi accelerated cosmic rays is less than 2, we expect a larger number of cosmic rays at a given energy to be produced the higher the Mach number of the shock.

6. Properties of the Scattered Ions

In this section the properties, in particular the number densities of the upstream scattered ions, are examined for 3 simulation runs with Alfvén Mach numbers of 5, 6, and 7. Simulations with higher Mach numbers were run in Quest (1987), but not long enough to achieve steady-state values for the upstream scattered ions (see below for the criterion used). The purpose of the exercise is to show that the scattered ion behavior is plausible, and lends itself easily to further acceleration.

The procedure for obtaining the densities was to first identify the position of the shock at $t = 200\Omega_i^{-1}$, and then select a point $x = x_S$ just upstream (roughly the center of the simulation box for all three runs) as the upper bound in x over which the upstream statistics would be accumulated. Four spatial intervals were then defined: region 1, closest to the shock, was defined to be between $x = 7x_S/8$ and x_S, region 2 was defined to be between $x = 3x_S/4$ and $x = 7x_S/8$, region 3 was between $x = x_S/2$ and $3x_S/4$, and region 4 was between $x = 0$ and $x_S/2$. Smaller intervals were not taken owing to the small number of scattered ions (between 100 - 250 macro-particles for each run). An ion upstream of the shock was defined to be "scattered" if it's speed in the plasma rest frame exceeded U_u.

The results are shown in Figure 6, where the scattered number density normalized to the far upstream density is plotted as a function of distance from the shock, normalized to the simulation box size. The squares correspond to the $M_A = 5$ run, the diamonds to $M_A = 6$, and the octagons to $M_A = 7$. A clear trend in all three cases is a decreasing number density with increasing distance from the shock, to be expected if the ions are being resonantly scattered by the upstream waves. An estimate of the exponentiation length D/U_u, where D is the spatial diffusion coefficient, was obtained by doing a least-squares-fit to the logarithmic data, and the results are shown in Figure 7. A probable upper bound to the expected diffusion coefficient is $2\pi\Omega_i/k^2$. Estimating the wavelength as $kc/\omega_{pi} \simeq 1/M_A$ obtains

$$\frac{\omega_{pi}D}{U_u c} \leq 2\pi M_A. \tag{6}$$

Referring back to Figure 7, the observed values of D are below the expected maximums, but still large, and suggestive of strong scattering upstream of the shock. Thus, not only do the waves confine the downstream plasma so that only a small fraction can escape back upstream, the majority (90%) of the upstream ions are turned back towards the shock by the self-generated upstream waves. Since the process of upstream reflection should result

in the energization of the ions, it follows that the mean energy should be substantially greater than the ram energy ($M_i U_s^2/2$).

The energy of the scattered ions can be calculated from the simulations, and the results show that, on the average, they are between 2-4 more energetic than the upstream background population. This result is consistent with the expected energy gain from a single reflection with the upstream waves, and demonstrates (in conjunction with the statements of the previous paragraph) that after a small group of ions is randomly scattered back upstream to maintain the generation of electromagnetic waves, these same ions are preferentially accelerated with great efficiency. By contrast, the the background population must supply the energy for both the waves and scattered particles and is therefore preferentially slowed. Since, however, the number of scattered ions is small, the drag on the background ions is only between $5 - 10\%$.

There are several caveats to the above estimates of the diffusion length. The number of particles per cell in the simulations upstream of the shock was $\simeq 20$. This means that the statistics for the scattered particles were poor, and the waves generated by them very noisy. A second problem is the implicit assumption that the densities of the scattered ions measured at time $t = \Omega_i^{-1}$ represent an average, or steady-state value. The number density and average x velocity of the background ions for runs with M_A's of 8, 9, and 10 (reported in Quest, 1987) were calculated and yielded values of the net flux (NU_x) which varied from the far upstream flux by better than 10%, indicating that the overall shock structure (in particular, the region upstream of the main ramp) was still evolving. This is plausible, since ions which escaped upstream at early times during the shock creation generated upstream waves for a good fraction (in time) of the simulation run. The runs with M_A's of 5 and 6 did much better in this regard, deviating from the upstream flux by less than 1%. These runs, however, were run twice as long as the higher Mach number cases. The $M_A = 7$ case lay somewhat between (a 4% deviation), but additional numerical difficulties with this run make it's reliability (at least for estimating the upstream diffusion length) difficult to calculate. Thus, while the results quoted above are encouraging, additional simulations with better resolution and longer run times will be required before reliable estimates of the injected particle distributions can be made.

7. Conclusions

In this paper a model for the structure of a high Mach number parallel shock has been outlined. It was argued that electromagnetic waves are a necessary part of the structure because acoustic waves cannot steepen into shocks unless the the electron to ion temperature ratio is very large and the Mach number is reasonably la Since the electromagnetic waves are convected through the shock at roughly the local plas. flow speed, it is necessary to generate them upstream. The generation is accomplished by continually scattering a small fraction of the background ions back into the upstream medium, driving a resonant electromagnetic beam instability. In the context of the shock structure, the sole function of the ions scattered back upstream is to generate the electromagnetic waves that ultimately provide the dissipation for the shock. As a side effect of the wave generation, however, the scattered ions are efficiently and selectively accelerated at the expense of the background

ions. In turn, a small fraction of these ions should be back-scattered again, generate new waves that further accelerate them, and cosmic ray generation by the first-order Fermi process will be a likely, nearly unavoidable, consequence. Because of limitations in the present simulations, however, this latter conclusion must be considered speculative. Better numerical models with higher resolution (more macro-particles) and longer runs will be required to make definitive statements concerning both the shock dissipation process and it's ability to accelerate ions to high energies.

Assuming that cosmic rays do result from the energetic ions produced by the shock dissipation process, there are additional questions that arise. Hydrodynamic calculations have shown that at high Mach numbers cosmic rays can form a shock wave of thickness D/U_s by absorbing the flow energy from the background ions, and therefore eliminate the "subshock" associated with the background ions (Drury et al., 1981; Axford et al., 1982). If the cosmic rays are self-generated by the shock, this would imply that after a sufficiently long time past the shock creation, the shock ramp would broaden, and background ions would no longer would be injected into the cosmic ray "pool". It follows that either a different mechanism of injection (other than the one discussed) would provide the seed ions, or that cosmic ray generation would be a cyclical process (a time-dependent shock structure). A second possibility (Eichler, 1979) is that the "subshock" never disappears, even at high Mach numbers, and that a steady-state structure is reached when cosmic ray injection and production is balanced by convective and other losses. Finally, there is the question of what happens when the shock is oblique. Clearly the shock dissipation mechanism is modified as the angle the magnetic field makes with the shock normal becomes more perpendicular. Additionally, the DC magnetic field jump and the time-independent electric field associated with it can lead to drift acceleration. Thus, the injection process becomes a complicated mixture of several mechanisms, and future research will need to address these issues.

Acknowledgements

This work was supported in part by the U.S.D O.E.

References

Achterberg, A., Modification of scattering waves and its importance for shock acceleration, *Astron. Astrophys., 119*, 274, 1983.

Armstrong, T. P., Shock drift acceleration, in *Collisionless Shocks in the Heliosphere: Reviews of Current Research*, eds. R. G. Stone and B. T. Tsurutani, AGU, Washington DC, 1985.

Arons, J., C. Max, and C. F. McKee, *Particle Acceleration Mechanisms in Astrophysics*, AIP Conference Proceedings No. 56, American Institute of Physics, New York, 1979.

Axford, W. I., The acceleration of cosmic rays by shock waves, *Proc. NY Acad. Sci., 375*, 297, 1981a.

Axford, W. I., The acceleration of galactic cosmic rays, in *Origin of Cosmic Rays*, eds. G. Setti, G. Spada, and A. W. Wolfendale, Reidel, Dorrecht, Holland, 1981b.

Axford, W. I., Acceleration of cosmic rays by shock waves, in *Plasma Astrophysics*, eds. Guyenne and Long, ESA, Paris, 1981c.

Axford, W. I., Leer, and G. Skadron, The acceleration of cosmic rays by shock fronts, *Plovdiv, 11*, 132, 1977.

Axford, W. I., E. Leer, and J. F. McKenzie, The structure of cosmic ray shocks, *Astron. Astrophys., 111*, 317, 1982.

Barnes, A., Theory of generation of bow-shock-associated hydromagnetic waves in the upstream interplanetary medium, *Cosmic Electrodyn., 1*, 90, 1970.

Bell, A. R. The acceleration of cosmic rays in shock fronts - I, *Mon. Not. R. Astron. Soc., 182*, 147, 1978.

Blandford, R. D., and J. P. Ostriker, Particle acceleration by astrophysical shocks, *Ap. J., 221*, L29, 1978.

Blandford, R. D., and L. L. Cowie, in *Supernovae and Supernovae remnants*, eds. M. J. Rees and R. Stoneham, Reidel, Holland, 1982.

Blandford, R. D., and D. Eichler, Particle acceleration at astrophysical shocks: a theory of cosmic ray origin, Phys. Lett., in press, 1987.

Cargill, P. J., C. C. Goodrich, and K. Papadopoulos, Interaction of two collisionless shocks, *Phys. Rev. Lett., 56*, 1986.

Chandrasekhar, S., A. N. Kaufman, and K. M. Watson, The stability of the pinch, *Proc. Roy. Soc. Ser. A, 245*, 435, 1958.

Drury, L. O'C., and H. J. Völk, Hydromagnetic shock structure in the presence of cosmic rays, *Astrophys. J., 248*, 344, 1981.

Drury, L. O'C., An introduction to the theory of diffusive shock acceleration of energetic particles in tenuous plasmas, *Rep. Prog. Phys.*, *46*, 973, 1983.

Eichler, D., Particle acceleration in collisionless shocks: regulated injection and high efficiency, *Ap. J.*, *229*, 419, 1979.

Ellison, D. C., Shock acceleration of diffuse ions at the earth's bow shock: acceleration efficiency and A/Z enhancement, *J. Geophys. Res.*, *90*, 29, 1985.

Ellison, D. C., and D. Eichler, Monte Carlo shock-like solutions to the Boltzmann equation with collective scattering, *Ap. J.*, *286*, 691, 1984.

Forman, M. A., and G. M. Webb, Acceleration of energetic particles, in *Collisionless Shocks in the Heliosphere: Reviews of Current Research*, eds. R. G. Stone and B. T. Tsurutani, AGU, Washington DC, 1985.

Forslund, D. W., and J. P. Freidberg, Theory of laminar collisionless shocks, *Phys. Rev. Lett.*, *27*, 1189, 1971.

Fried, B. D., and R. W. Gould, Longitudinal ion oscillations in a hot plasma, *Phys. Fluids*, *4*, 139, 1961.

Gary, S. P., The electromagnetic ion beam instability and energy loss of fast alpha particles, *Nucl. Fusion*, *18*, 327, 1978.

Gary, S. P., Microinstabilities upstream of the earth's bow shock: A brief review, *J. Geophys. Res.*, *86*, 4331, 1981.

Golden, K. I., L. M. Linson, and S. A. Mani, Ion streaming instabilities with application to collisionless shock wave structure, *Phys. Fluids*, *16*, 2319, 1973.

Goodrich, C. C., and J. D. Scudder, The adiabatic energy change of plasma electrons and the frame dependence of the cross-shock potential at collisionless magnetosonic shock waves, *J. Geophys. Res.*, *89*, 6654. 1984.

Harned, D. S., Quasineutral hybrid simulation of macroscopic plasma phenomena, *J. Comp. Phys.*, *47*, 452, 1982.

Jackson, R. W., Second-order effects related to a model for a parallel shock, *J. Geophys. Res.*, *88*, 9981, 1983.

Kan, J. R., and D. W. Swift, Structure of the quasi-parallel bow shock: Results of numerical simulations, *J. Geophys. Res.*, *88*, 6919, 1983.

Kennel, C. F., and R. Z. Sagdeev, Collisionless shock waves in high β plasmas, 1, *J. Geophys. Res.*, *72*, 3303, 1967.

Kennel, C. F., J. P. Edmiston, and T. Hada, A quarter century of collisionless shock research, in *Collisionless Shocks in the Heliosphere: A Tutorial Review*, eds. R. G. Stone and B T. Tsurutani, AGU, Washington DC, 1985.

Kovner, M. S., Instability of low-frequency electromagnetic waves in a plasma traversed by

a beam of charged particles, *J. Exptl. Theoret. Phys. (English Translation), 13*, 369, 1961.

Lee, M. A., Coupled hydromagnetic wave excitation and ion acceleration upstream of the earth's bow shock, *J. Geophys. Res., 87*, 5063, 1982.

Mason, R. J., Structure of evolving ion-acoustic fronts in collisionless plasmas, *Phys. Fluids, 13*, 1042, 1970.

Mason, R. J., Computer simulation of ion-acoustic shocks. The diaphragm problem, *Phys. Fluids, 14*, 1943, 1971.

Melrose, D., B., *Plasma Astrophysics, vol 2*, Gordon and Breach, New York, 1980.

Moiseev, S. S., and R. Z. Sagdeev, Collisionless shock waves in a plasma in a weak magnetic field, in *Plasma Physics. J. Nucl. Energy, Part C, 5*, 43, 1963.

Parker, E. N., *Phys. Rev., 109*, 1328, 1958.

Parker, E. N., A quasi-linear model of plasma shock structure in a longitudinal magnetic field, *J. Nuclear Energy, C2*, 146, 1961.

Quest, K. B., Simulation of quasi-parallel collisionless shocks, in *Collisionless Shocks in the Heliosphere: Reviews of Current Research*, ed. B. T. Tsurutani and R. G. Stone, AGU, 1985.

Quest, K. B., Theory and simulation of collisionless parallel shocks, *J. Geophys. Res.*, submitted, 1987.

Scholer, M., Diffusive acceleration, in *Collisionless Shocks in the Heliosphere: Reviews of Current Research*, eds. R. G. Stone and B. T. Tsurutani, AGU, Washington DC, 1985.

Sentman, D. D., J. P. Edmiston, and L. A. Frank, Instabilities of low frequency parallel propagating electromagnetic waves in the earth's foreshock region, *J. Geophys. Res., 86*, 7487, 1981.

Thomsen, M. F., Upstream suprathrmal ions, in *Collisionless Shocks in the Heliosphere: Reviews of Current Research*, ed. B. T. Tsurutani and R. G. Stone, AGU, 1985.

Thomas, V. A., and S. H. Brecht, Simulation of magnetic phenomena driven by parallel ion motion, *Phys. Fluids, 29*, 3398, 1985.

Tidman, D. A., and N. A. Krall, Shock waves in collisionless plasmas, Wiley-Interscience, New York, 1971.

Winske, D., and M. M. Leroy, Diffuse ions produced by electromagnetic ion beam instabilities, *J. Geophys. Res., 89*, 2673, 1984.

Zachary, A., Resonant Alfvén wave instabilities driven by streaming fast particles, Ph.D. Thesis, Lawrence Livermore National Laboratory, University of California, California, 1987.

Figure Captions

Figure 1. Evolution of parallel shock structure starting from a Rankine-Hugoniot state. The left column of figures is the ion phase space V_x normalized to the shock speed U_u. The right column is the transverse magnetic field component B_y normalized to the far upstream field magnitude B_u. Both the phase space and magnetic field are plotted against position normalized to the upstream ion inertial length c/ω_{pi}. The column of numbers at far right is the time in units of inverse in cyclotron frequency Ω_i^{-1}. The parameters of the shock are $M_A = 5$, upstream $\beta = 1.5$, and upstream $T_i/T_e = 0.5$.

Figure 2. Minimum Mach number for which the firehose criterion is attained downstream of a parallel shock, plotted as a function of total upstream β, and assuming upstream $T_i/T_e = 0.5$. In the upper panel the magnetosonic Mach number M_s is plotted, and in the lower panel the Alfvén Mach number M_A is used. The shaded areas in the plots correspond to switch-on shocks (lower-left corner) and sub-sonic flow (lower-right corner).

Figure 3. Ion phase space for $M_A = 5$, $T_i/T_e = 0.5$, and $\beta = 1.5$ parallel shock, plotted against position, at time $t\Omega_i = 200$. The velocities V_x, V_y, and V_z are all normalized to the shock speed U_u.

Figure 4. Magnetic field as a function of position for same shock and time as in Figure 3. The magnetic field is normalized to the far upstream field magnitude B_u.

Figure 5. Two components of ion phase space, density, and y component of magnetic field, plotted against position for same shock as described in previous two figures. Note that the spatial scale is greatly expanded relative to Figures 3 and 4.

Figure 6. number density of reflected ions N_r, normalized to far upstream density N_u, as a function of distance from the shock. The squares correspond to the $M_A = 5$ run, the diamonds to $M_A = 6$, and the octagons to $M_A = 7$, All three cases calculated at time $t\Omega_i = 200$. X_{max} is the length of the simulation box, and was 600, 720, and $840c/omega_{pi}$, for $M_A = 5$, 6, and 7, respectively.

Figure 7. Calculation of the exponentiation length of the reflected ion number densities described in Figure 6. The values were obtained by doing a least-squares fit through each of the three sets of the 4 logarithmic data points displayed in the previous figure. The dotted line is a least-squares fit to the data that makes the figure look better, but otherwise serves no function.

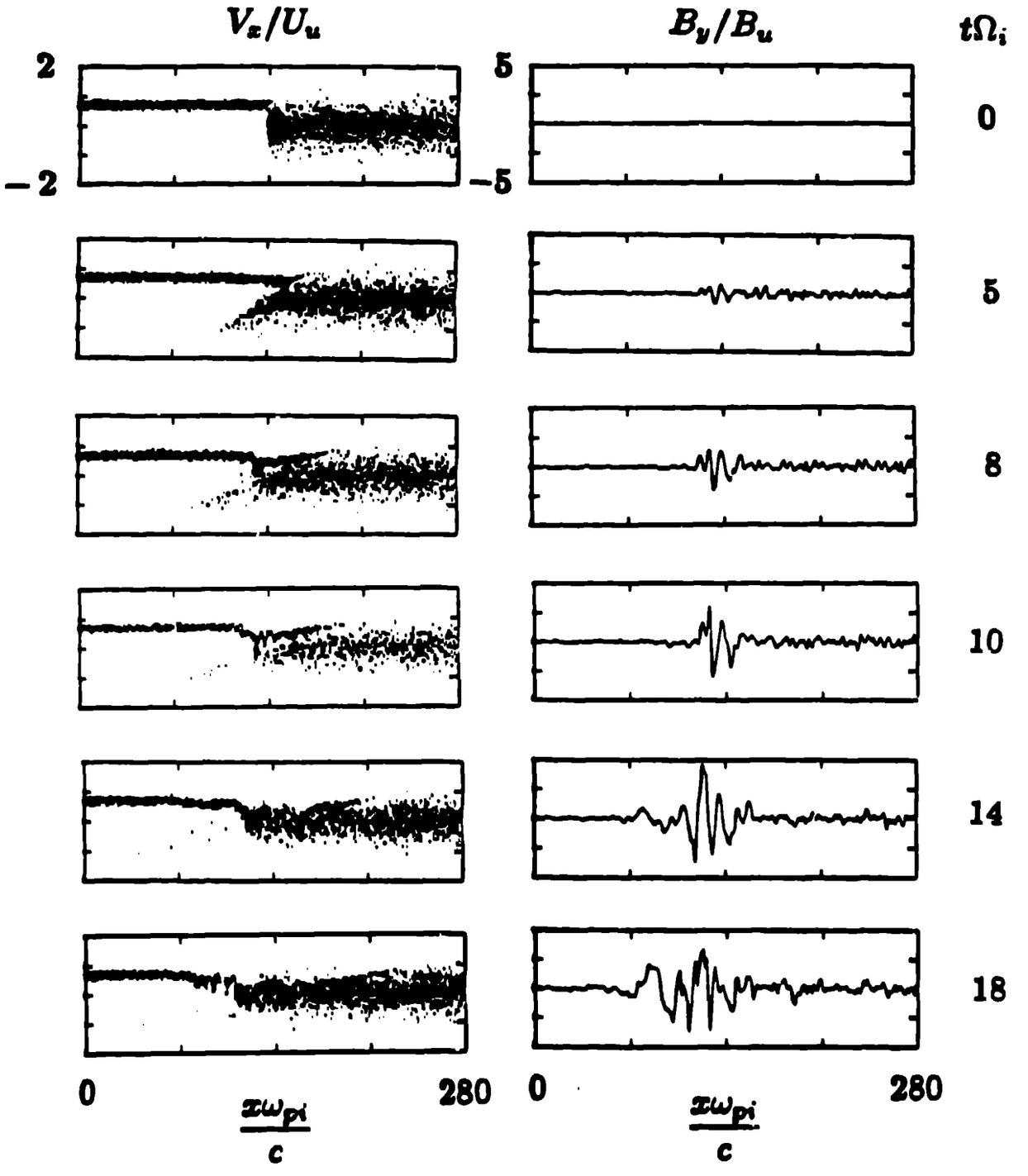
V_x/U_u
B_y/B_u
$t\Omega_i$
2
−2
5
−5
0
5
8
10
14
18
0
280
0
280
$\frac{x\omega_{pi}}{c}$
$\frac{x\omega_{pi}}{c}$

Figure 1

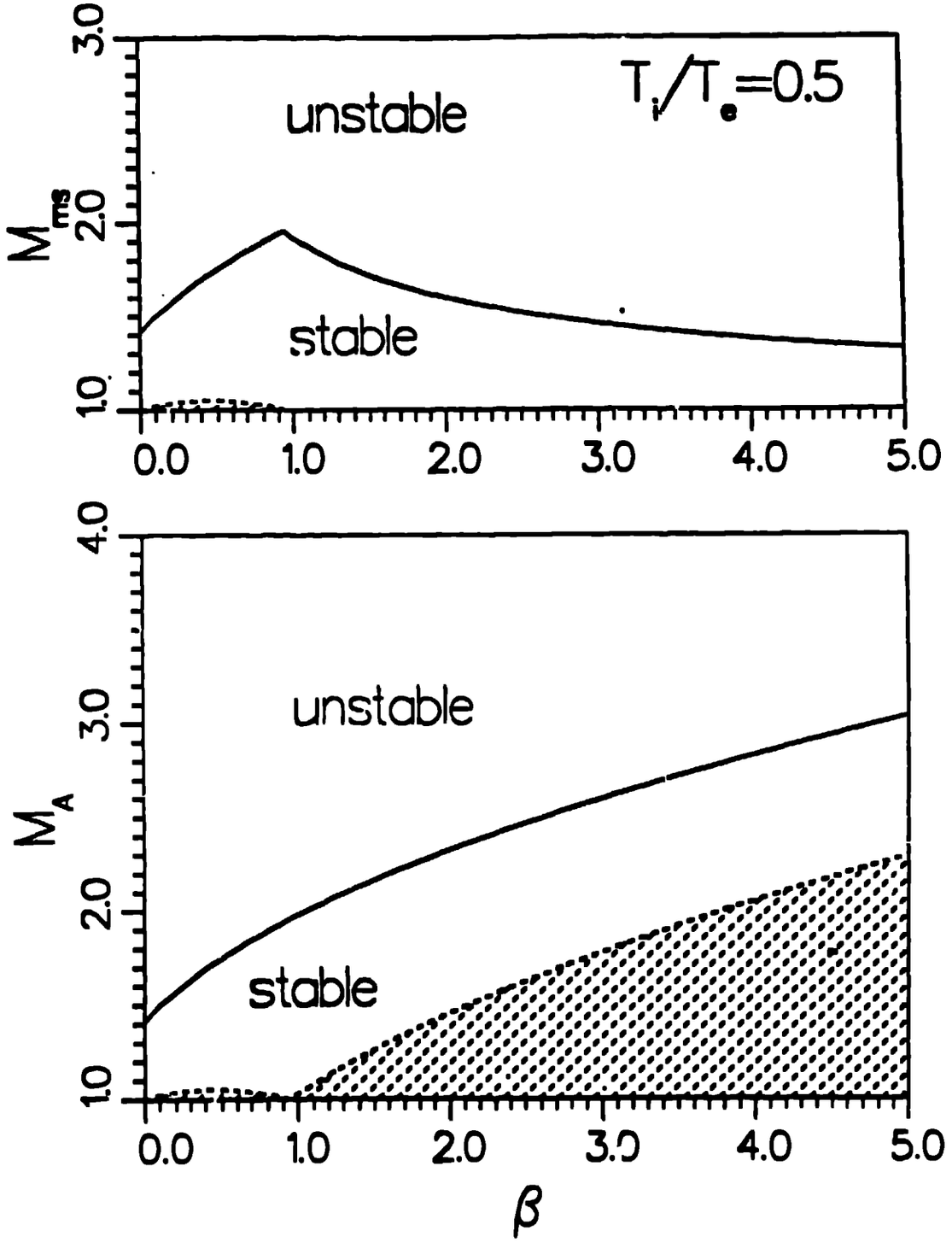
3.0
2.0
1.0
M_{ms}
unstable
T_i/T_e=0.5
stable
0.0
1.0
2.0
3.0
4.0
5.0
4.0
3.0
2.0
1.0
M_A
unstable
stable
0.0
1.0
2.0
3.0
4.0
5.0
β

Figure 2

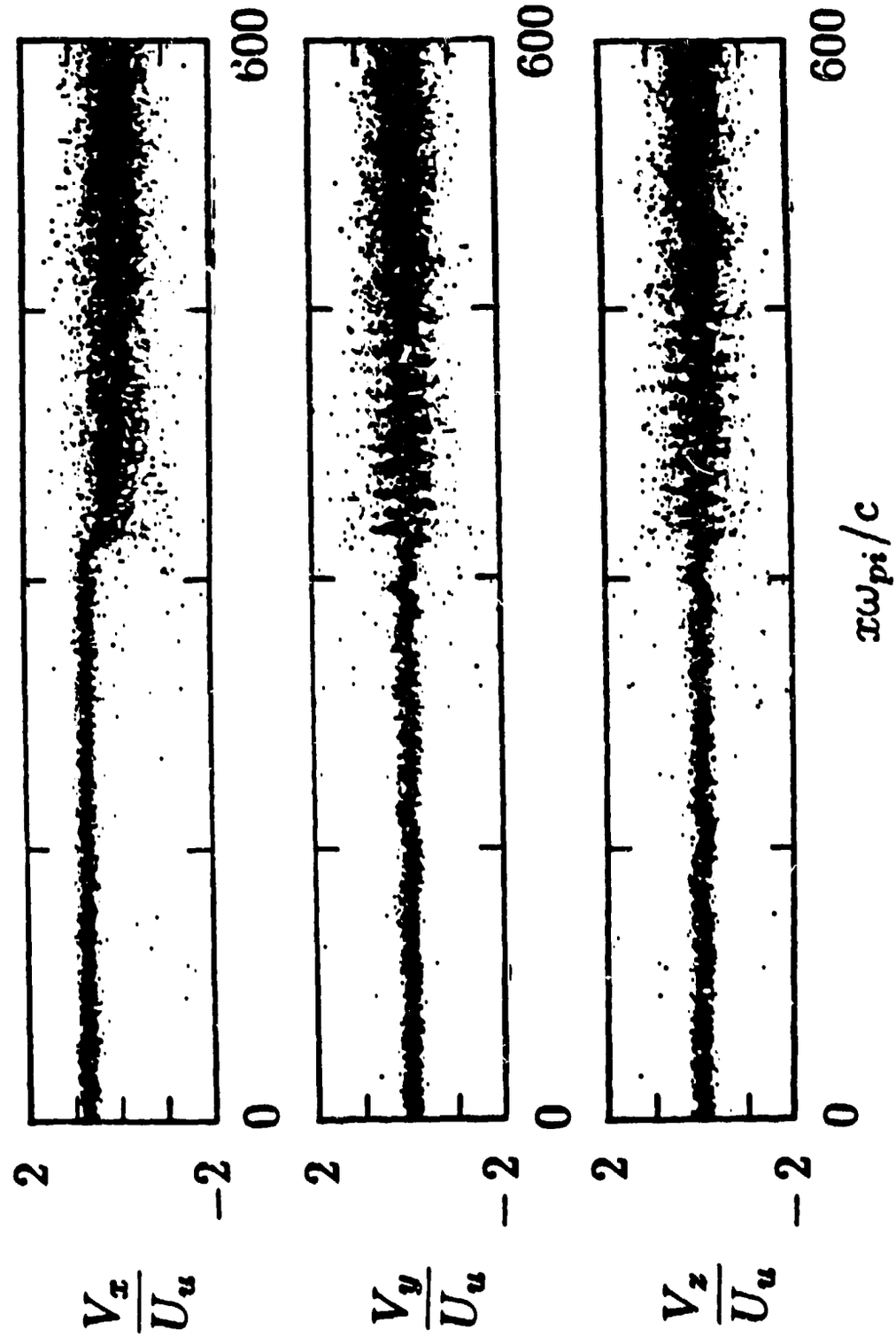

Figure 3

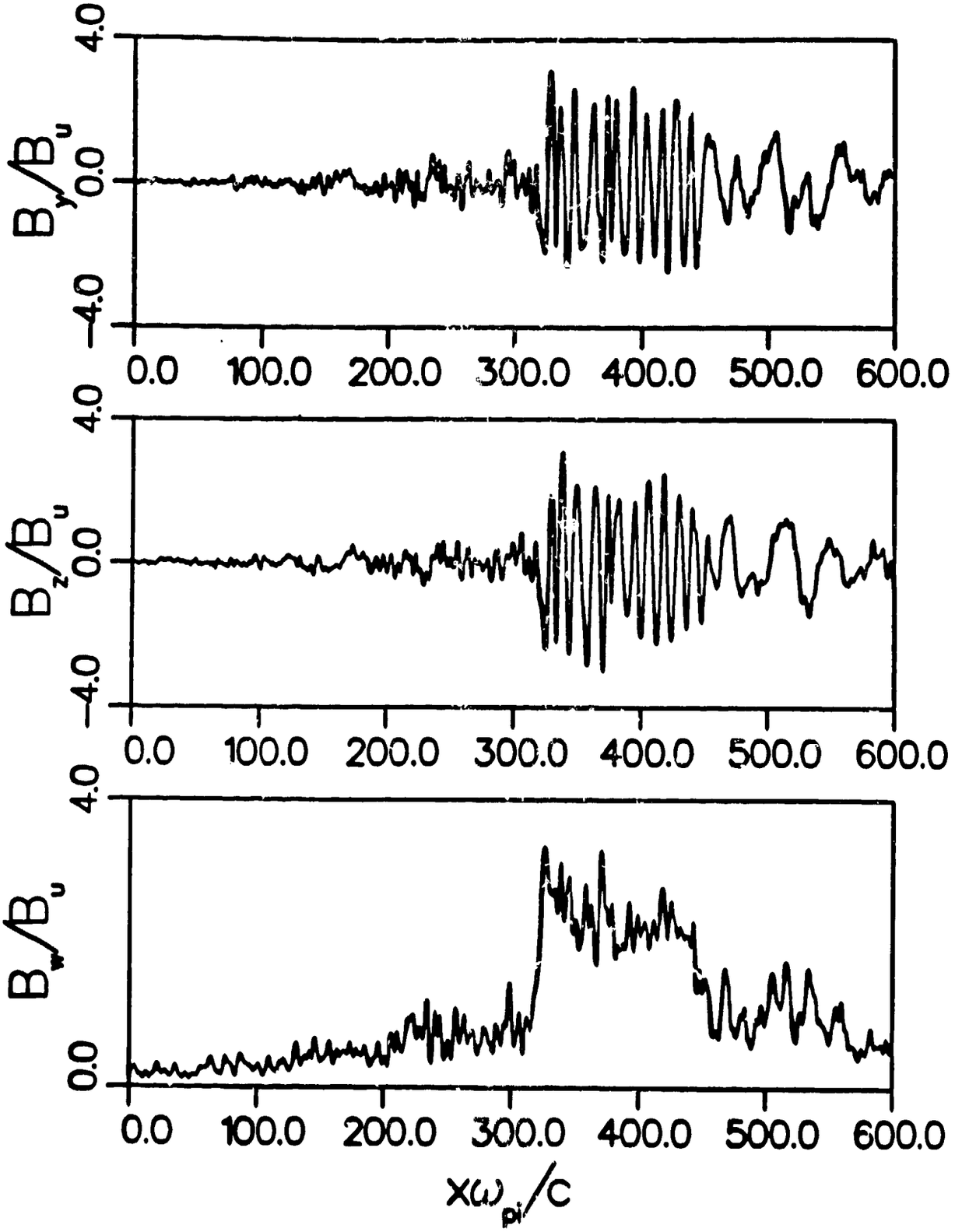
B_y/B_u
4.0
0.0
-4.0
0.0
100.0
200.0
300.0
400.0
500.0
600.0
B_z/B_u
4.0
0.0
-4.0
0.0
100.0
200.0
300.0
400.0
500.0
600.0
B_w/B_u
4.0
0.0
0.0
100.0
200.0
300.0
400.0
500.0
600.0
$X\omega_{pi}/C$

Figure 4

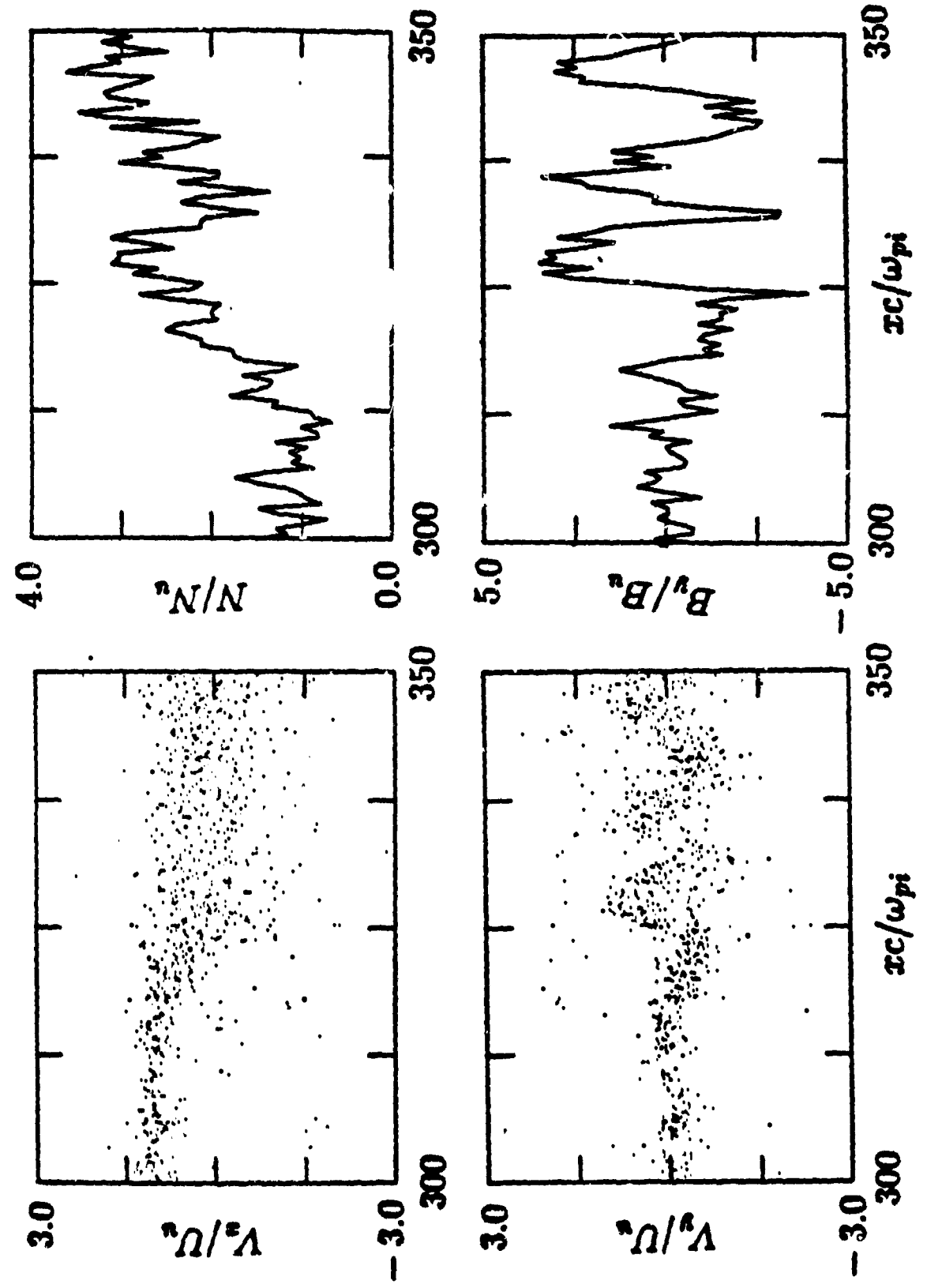

Figure 5

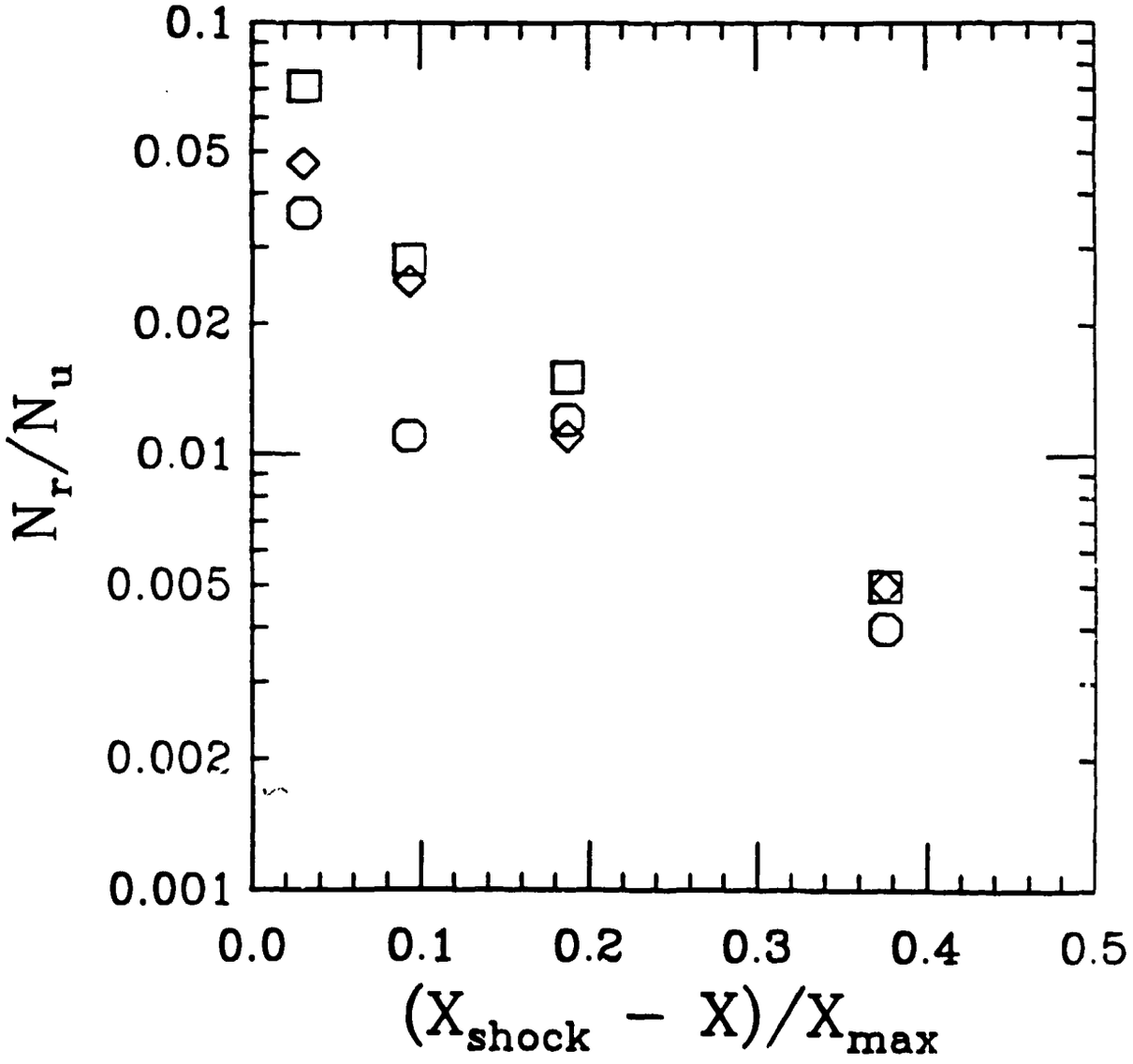
0.1
0.05
0.02
0.01
0.005
0.002
0.001
N_r/N_u
0.0
0.1
0.2
0.3
0.4
0.5
$(X_{shock} - X)/X_{max}$

Figure 6

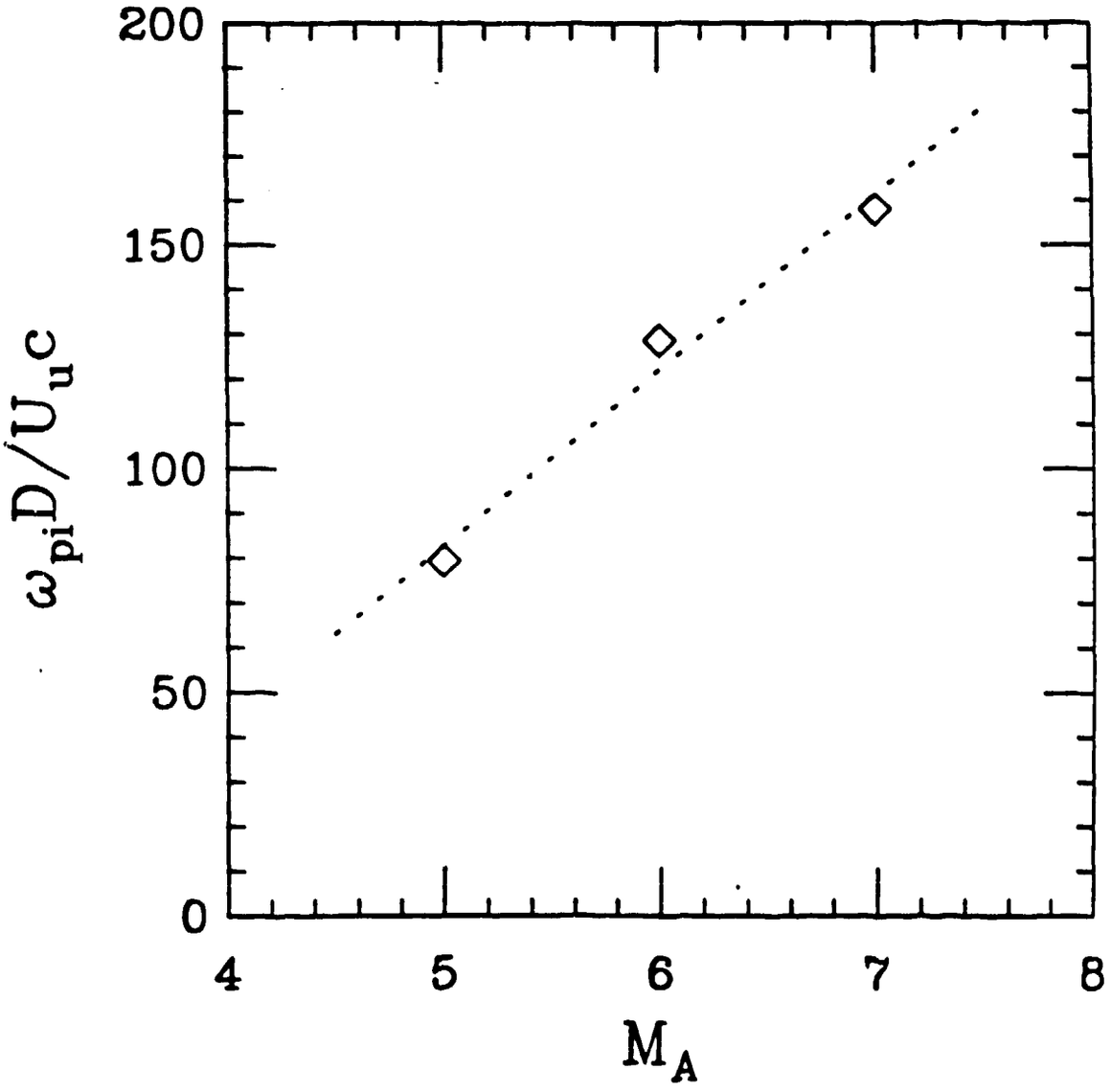

Figure 7